

AN ANALYTICAL MODEL OF INTERGRANULAR CREEP CRACKING.
 APPLICATION TO PRECIPITATION-HARDENED Al ALLOYS EMBRITTLED BY Pb.
 B. QUANTIN^{*1} and M. GUTTMANN^{*2}

An analytical model has been developed to account for the kinetic evolution of crack populations in creeping alloys. Its application to measured crack distributions in precipitation hardened Al-base alloys embrittled by Pb leads to simple equations for crack growth $v(x)$ and nucleation rate $g(t)$ as functions of time t and crack length x :

$$v(x) = v_1 x \quad g(t) = g_0 [1 - \exp \alpha(t - t_0)]$$

These equations allow the influence of microstructural and compositional variables and of creep conditions on intergranular damage to be analysed through their effects on the parameters v_1 and g_0 .

INTRODUCTION

Creep damage has generally been thought of as occurring by either of two distinct processes, wedge-type cracks and cavities. Moreover, the majority of microscopic models for creep cracking only take into account a single, semi-infinite, plane crack, ignoring deflections at triple junctions, and those for cavitation consider the evolution of either a single cavity or that of a uniformly distributed population of identical cavities.

Recent work has shown, however that these two types of damage often correspond to two different scales or stages of a single damage process, since cavitation was observed to develop at the tip of advancing cracks (1-6), and models were proposed to explain this behaviour (7-10). However these microscopic models do not take into account the experimental fact that creep damage takes the form of a non-uniform distribution of defects, cavities and/or cracks, which may therefore develop unevenly according to their size and the local values of other parameters.

In view of the complexity of these relationships, phenomenological models can be of some help in describing the kinetic evolution of a defect population, concurrently with physical models which shed light on the elementary mechanisms but overlook the statistical aspect of creep damage.

*Centre des Matériaux de l'Ecole des Mines, Evry, France ;

1 present address : Cabinet Rinuy-Santarelli, 14 Avenue de la Grande Armée, 75016 Paris, France.

2 present address : Electricité de France, Département EMA, Les Renardières, 77250 Moret-sur-Loing, France.

EXPERIMENTAL DETAILS

In a study (6,11,12) of creep embrittlement of precipitation-hardened 6060-type Al-Mg-Si alloys by an insoluble impurity, Pb, a quantitative experimental analysis of intergranular cracking was carried out by optical microscopy on four heats containing up to 164 ppm Pb.

The partial densities of cracks were empirically defined as the numbers ρ_n^{Δ} of cracks per unit area of longitudinal sections having a length in the interval $[n\Delta - \frac{\Delta}{2}, n\Delta + \frac{\Delta}{2}]$, where n was an integer and Δ , the width of all crack classes, corresponded to one division of the micrometer, $\Delta = 5.75 \mu\text{m}$. It was considered that the detection limit of the technique was about $\Delta/2$, which is the size of large inclusions and large intragranular cavities (6) with which the incipient cracks might be mistaken. Defects shorter than $\Delta/2$ were thus ignored in the analysis.

Although a drastic decrease in creep life with increasing applied stress and Pb content was straightforwardly observed (6) no simple relationship could be established between creep cracking characteristics and macroscopic rupture properties ($\dot{\epsilon}_m, \sigma_r, t_r, \epsilon_r$, etc) or Pb content (11,12). An analytical model of cracking, based on statistically significant data ($\approx 120\ 000$ cracks counted and classified over 76 testpieces) was therefore developed in order to isolate the incidences of the various parameters.

GENERAL MODEL

The observed micro-mechanism of crack growth

A phenomenological model of creep-crack distribution evolution has already been developed by Lindborg (13), based on the observation that the majority of intergranular cracks were arrested at triple junctions at both ends, which implied that growth was virtually instantaneous along individual grain boundary facets, and was controlled essentially by re-nucleation beyond triple junctions. Lindborg's probabilistic rationale, well suited to that discontinuous type of growth, is not compatible with the mode of crack growth in the present Al-base alloys, where the cracks advance by absorbing very small ($\leq 0.3 \mu\text{m}$) cavities which develop immediately ahead (i.e. within a few μm) of their tip (6). This microscopic mechanism explains that crack growth is continuous at the scale of grain facets and is not basically controlled by arrest at triple junctions, resulting in the fact that more than 2/3 of the observed cracks have at least one of their ends between two triple junctions: crack distributions, fig. 1-b, do not exhibit maxima when the crack length, expressed in terms of number of grain boundary facets, is an integer, and the absolute maximum is for cracks smaller than one facet. Conversely, the crack density continuously decreases with increasing crack length when the latter is measured in absolute (metric) units, fig. 1-a, starting from a minimum value Δ related to the detection limit $\Delta/2$. Thus, only the latter type of distribution has been considered, and a continuum model had to be developed to account for the optical microscopy observations.

Hypotheses of the model

a - Coalescence of, and interaction between, individual cracks are neglected, which is reasonable in view of the small absolute density of cracks even at rupture (11).

b - The growth rate v of an individual crack in a given alloy for given heat treatment and testing conditions is essentially a function of its length x . In most of the microscopic models of crack growth, v is found to increase as K^m , where K is the applied stress intensity factor, proportional to $x^{1/2}$, and m is a constant. Therefore $v(x)$ is assumed to have the form :

$$v(x) = \frac{dx}{dt} = v_q x^q \quad (\text{growth equation}) \quad (1)$$

where $q = m/2$. When vacancy diffusion is responsible for crack growth and crack tip stress concentrations are not neglected as in ref. 14,15, $2 \leq m \leq 4$ (8,9,10) and thus $1 \leq q \leq 2$. When crack extension is controlled solely by plastic deformation, m becomes equal to the stress component of the creep law $\dot{\epsilon} = A\sigma^m$ and can therefore be much larger (7). Experimental values ranging between 3 and 30 have been obtained (16).

c - The partial crack density at time t , $\rho(x,t)$, is an analytical function of x and t whose values at $x = n\Delta$ are related to the experimentally measured ρ_n^Δ by the equation :

$$\rho(n\Delta, t) = \rho_n^\Delta / \Delta \quad (2)$$

d - Only an empirical acceptance of nucleation is implied here : the "nucleation rate" $g^\Delta(t)$ is considered as the number of cracks which become detectable, i.e. longer than $\Delta/2$, per unit time. The same convention, reminded by the superscript Δ , applies to the total density $\rho^\Delta(t)$ and integrated length $\mathcal{L}^\Delta(t)$ of cracks per unit area at time t .

Basic equations of the model

The possibility of crack sintering being outruled, $v(x) \geq 0$ and the ranking of existing cracks according to their length remains unchanged during growth. Therefore the number of cracks having their lengths in the interval $[x - \frac{\Delta}{2}, x + \frac{\Delta}{2}]$ at time t , will be found unchanged in the interval $[(x - \frac{\Delta}{2}) + v(x - \frac{\Delta}{2})dt, (x + \frac{\Delta}{2}) + v(x + \frac{\Delta}{2})dt]$ at time $t + dt$. This yields the distribution equation, which is formally identical to a conservation equation :

$$\frac{\partial \rho}{\partial t} + \frac{\partial}{\partial x} (v \cdot \rho) = 0 \quad (3)$$

Similarly, the "nucleation" rate is equal to the number of cracks whose lengths grow over $\Delta/2$ per unit time :

$$g^\Delta(t) = v(\frac{\Delta}{2}) \cdot \rho(\frac{\Delta}{2}, t) \quad (4)$$

The incubation time t_0 is that at which the first crack becomes detectable (i.e. $x = \Delta/2$). Under the above assumptions, this crack will remain the longest one throughout creep life. Its length x_{max} at time t is related to t by the equation :

$$t - t_0 = \int_{\Delta/2}^{x_{max}} [v(x)]^{-1} dx \quad (5)$$

The total density and length of cracks can be calculated by :

$$\rho^\Delta(t) = \int_{\Delta/2}^{x_{max}} \rho(x,t) dx \quad (6)$$

$$\mathcal{L}^\Delta(t) = \int_{\Delta/2}^{x_{max}} x \rho(x,t) dx \quad (7)$$

Eleven boundary conditions can be written :

$$\forall t, t_0 \leq t < t_r : \quad g^\Delta(t) > 0 ; \rho^\Delta(t) > 0 ; \mathcal{L}^\Delta(t) > 0 \quad (8)$$

$$\forall t, t_0 \leq t < t_r ; \forall x, \frac{\Delta}{2} \leq x \leq x_{\max} :$$

$$\rho \geq 0 ; \frac{\partial \rho}{\partial t} \geq 0 ; \frac{\partial \rho}{\partial x} \leq 0 ; \frac{\partial^2 \rho}{\partial x^2} \geq 0 \quad (9)$$

$$\rho(\frac{\Delta}{2}, t_0) = \rho^{\Delta}(t_0) = \rho^{\Delta}(t_0) = 0 \quad (10)$$

$$\rho(x_{\max}, t) = 0 \quad (11)$$

Among these, conditions (9) are imposed to comply with the shape and time dependence of the ρ vs. x curves, fig. 1-b. In particular the condition on curvature is strictly valid for large x only.

Resolution of the equations

Integration of the growth equation 1 yields :

$$x = (\frac{\Delta}{2}) \cdot \exp[v_q(t - t_i)/q] \quad (12)$$

where t_i is the time at which a given crack is first detected i.e. $x_i = \Delta/2$. For the first crack $t_i = t_0$ and $x = x_{\max}$, eqn. 5.

A general solution of eqn. 3 with separated variables has been obtained (11), using the above expression of $v(x)$, eqn. 1 :

$$\rho(x, t) = (g_0/v_q) x^{-q} \{1 - \exp[\alpha(t - t_0) - C\beta(x)]\} \quad (13)$$

where g_0 , α and C are constants,

$$C = (\alpha/v_q) (\Delta/2)^{1-q} \quad (14)$$

and $q \neq 1 \quad \beta(x) = (1-q)^{-1} [(2x/\Delta)^{1-q} - 1] \quad (15-a)$

$$q = 1 \quad \beta(x) = \ln(2x/\Delta) \quad (15-b)$$

The "nucleation" rate and the total density of cracks as defined by eqns. 4 and 6 have the expressions :

$$g^{\Delta}(t) = g_0 \{1 - \exp[\alpha(t - t_0)]\} \quad (16)$$

$$\rho^{\Delta}(t) = g_0(t - t_0) + (g_0/\alpha)\{1 - \exp[\alpha(t - t_0)]\} \quad (17)$$

Condition (11) leads to the time dependence of x_{\max} :

$$\alpha(t - t_0) = C\beta(x_{\max}) \quad (18)$$

The whole set of conditions (8-11) essentially reduces to (11) :

$$\alpha \cdot g_0 < 0 \quad (19-a)$$

$$q > 1 \quad |C| \leq 3q \quad (19-b)$$

The basic condition eqn.19-a decomposes into two cases, fig.2 :
 a - If $\alpha > 0$ and $g_0 < 0$, the "nucleation" rate and crack density increase exponentially with time, eqns. 16,17, and the majority of cracks are formed at the end of creep life. This behaviour is expected in case of essentially strain-controlled creep damage, which dominates at high stresses and creep rates.

b - If $\alpha < 0$ and $g_0 > 0$, $g^{\Delta}(t)$ tends asymptotically towards a constant value g_0 which then has the simple physical meaning of a steady state "nucleation rate". Accordingly, the total density of cracks $\rho^{\Delta}(t)$ tends to become linear with time :

$$\rho^{\Delta}(t) \rightarrow g_0(t - t_0) \quad (20)$$

The time necessary to establish this steady state regime is of the order of $1/\alpha$.

APPLICATION OF THE MODEL TO Al-Mg-Si ALLOYS

The observed variations of total crack density with time, fig. 3-a, being virtually linear (for 65 and 164 ppm Pb), at least after a certain time (for 29 ppm Pb), imply that $\alpha < 0$ and $g_0 > 0$ in the alloys and creep conditions considered ($T = 373 \text{ K} \approx 0.45 T_m$; $\sigma = 140$ to 210 MPa). These linear plots also imply that the exponential in eqn. 17 has become negligible, and, since $\beta(x)$ increases with x and C is negative (as α), eqn. 13 is equivalent to :

$$\rho(x, t) \approx (g_0/v_q)x^{-q} = B_q x^{-q} \quad (21)$$

for short cracks. Similarly, according to eqn. 2 :

$$\rho_n^\Delta(n, t) \approx B_q \Delta^{1-q} n^{-q} \quad (22)$$

Considering experimentally determined histograms of ρ_n^Δ , fig. 4, it appears that $q = 1$ is the best value consistent with the results for the lower values of n , i.e. in the range where the approximation of eqn. 21 applies. Only a few values of ρ_n^Δ appear somewhat erratic, due to the difficulty in identifying the smallest cracks. These conclusions hold for all the results obtained with 76 specimens of 4 alloys in 3 heat treatment conditions, and creep times ranging from 6 to 1 800 h (11,12).

The value $q = 1$ is consistent with the predictions of models of crack advance involving vacancy diffusion-controlled growth of cavities ahead of crack tip (8,9), i.e. $v \propto K^2$ for the larger stress intensity factors, and with our experimental observations which reveal the importance of diffusion processes in the creep-rupture of these alloys (6,11,12) :

- cavities are themselves divided into smaller vacuoles bounded by simple cristallographic planes, as occurs in the surface diffusion-controlled formation of equilibrium cavities ; this causes the surfaces of freshly formed cracks to appear pitted at an extremely fine scale ($\leq 0.1 \mu\text{m}$), see fig. 5 of ref. 6 ;
- later on, these fine features smooth out by surface diffusion ;
- the embrittling effect of Pb is enhanced as the creep rate is decreased, i.e. as time dependent mechanisms are allowed to prevail ;
- Auger electron spectroscopy has demonstrated that Pb rapidly covers fracture surfaces by surface diffusion even at low temperatures ; this is probably the basic mechanism of embrittlement.

The influence of microstructural and compositional variables upon "nucleation" and growth can be assessed by considering their effects on the parameters v_1 and g_0 of the model. g_0 is the slope of the straight lines in fig. 3-a, and B_1 can be graphically determined in fig. 4 with the help of eqn. 22. Then $v_1 = g_0/B_1$. The log-log plots of v_1 and g_0 vs. the minimum creep rate $\dot{\epsilon}_m$, fig. 5, reveal that remarkable correlations of the type

$$v_1 = v_1^0 (\dot{\epsilon}_m)^r \quad g_0 = g_0^0 (\dot{\epsilon}_m)^s \quad (23)$$

hold over 4 orders of magnitude of $\dot{\epsilon}_m$, which emphasizes the importance of plastic creep deformation process in crack nucleation and growth. The parameters v_1^0 , g_0^0 , r and s are characteristic of the material condition. Both v_1^0 and g_0^0 increase with increasing Pb content (11,12), which implies that both "nucleation" and growth are enhanced by the embrittling impurity. A decrease in grain size strongly increases B_1 by favoring "nucleation" (g_0 increases) and hindering growth (v_1 decreases). In the precipitation-hardened conditions, v_1 , g_0 and B_1 are virtually independent of aging time and Mg content, which implies that, for a given type of micro-

structure, crack nucleation and growth are not affected by hardness intrinsically but only via its effect on creep rate.

In the case $q=1$, simple equations relating v_1 and g_0 to x_{\max} can be established by combining eqns. 14, 15-a and 18 :

$$v_1(t-t_0) = \ln(2x_{\max}/\Delta) \quad (\text{cf. eqn. 12}) \quad (24)$$

$$g_0(t-t_0) = B_1 \ln(2x_{\max}/\Delta) \quad (25)$$

Numerical values of v_1 and g_0 can be consistently deduced from $\ln(x_{\max})$ vs. t plots, but this often leads to negative values of t_0 , as expected from fig. 4. In the present model, negative incubation times allow to account formally for the existence of defect nuclei prior to the onset of creep, as can be induced by cold work (17), or for a regime of intense nucleation during loading or primary creep (18), as depicted schematically in fig. 6.

CONCLUDING REMARKS

Due to its general character, the model is applicable to a variety of materials, provided a number of crack distributions are known experimentally. These are necessary to identify the parameters, beginning with the sign of α , which allows to choose between type a ("tertiary" cracking) or type b ("continuous" cracking) behaviours as depicted in fig. 2, and the value of q which may depend on the material type and on the ranges of temperature and applied stress. Even though they appear quite intricate in the raw experimental results, the influences of the various microstructural-compositional parameters and of creep conditions upon the cracking and thus on the rupture-life behaviours, lend themselves to a more straightforward analysis when the model equations and their parameters (g_0 , v_1 and probably α in other cases) are used, despite the simplicity of the initial assumptions of the model.

REFERENCES

1. Argon, A.S., Chen, I.W., and Lau, C.W., 1980, "Creep-Fatigue-Environment Interactions", TMS-AIME, Milwaukee, p. 46.
2. Gooch, D.J., 1977, *Mat. Sci. Eng.* **27**, 57 and **29**, 227.
3. Neate, G.J., 1977, *Engng. Fract. Mech.*, **9**, 297.
4. Sadananda, K., and Shahinian, D., 1977, *Metall. Trans. A*, **8A**, 439 and 1978, **9A**, 79.
5. Goods, S.H., and Nix, W.D., 1978, *Acta Metall.*, **26**, 739.
6. Guttman, M., and Quantin, B., 1982, *Metal Sci.*, **16**, in press.
7. Dimelfi, R.J., and Nix, W.D., 1977, *Int. J. Fract.*, **13**, 341.
8. Vitek, V., and Wilkinson, D.S., 1979, *ICSM* **5**, vol. 1, p. 321.
9. Raj, R., and Baik, S., 1980, *Metal Sci.*, **14**, 385.
10. Vitek, V., 1980, *Metal Sci.*, **14**, 403.
11. Quantin, B., 1981, Doctorat d'Etat Thesis, Université Paris-Sud.
12. Quantin, B., and Guttman, M., to be published.
13. Lindborg, U., 1969, *Acta Metall.*, **17**, 157.
14. Beeré, W., and Speight, M.V., 1978, *Metal Sci.*, **12**, 593.
15. Speight, M.V., Beeré, W., and Roberts, G., 1978, *Mat. Sci. Eng.*, **36**, 155.
16. Van Leeuwen, H.P., 1977, *Engng. Fract. Mech.*, **9**, 951.
17. Dyson, B.F., and Rodgers, M.J., 1974, *Metal Sci.*, **8**, 261.
18. Wilkinson, D.S., Abiko, K., Thyagarajan, N., and Pope, D.P., 1980, *Metall. Trans. A*, **11A**, 1827.

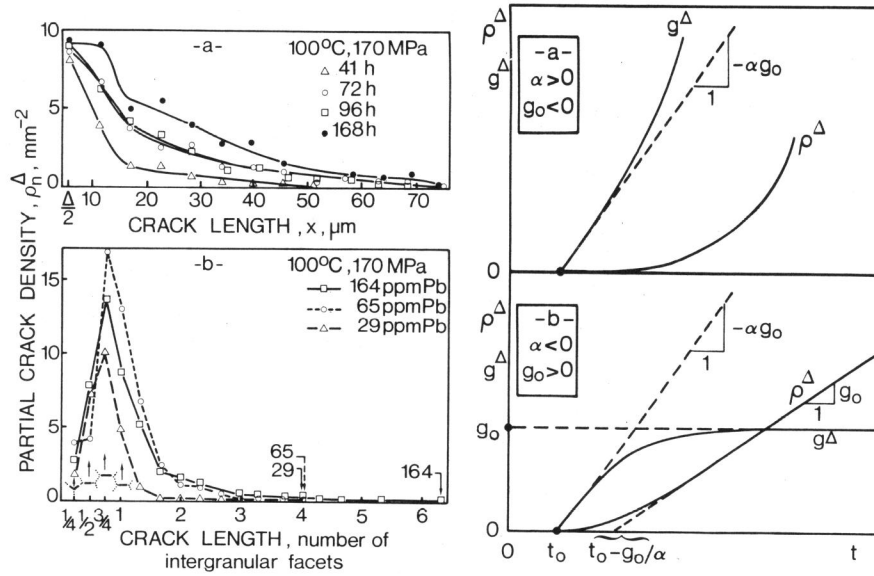


Figure 1 Examples of crack distribution in terms of : a - absolute length ; b - number of cracked intergranular facets.

Figure 2 Schematic of predicted $\rho^\Delta(t)$ and $g^\Delta(t)$ curves with the condition $\alpha \cdot g_0 < 0$.

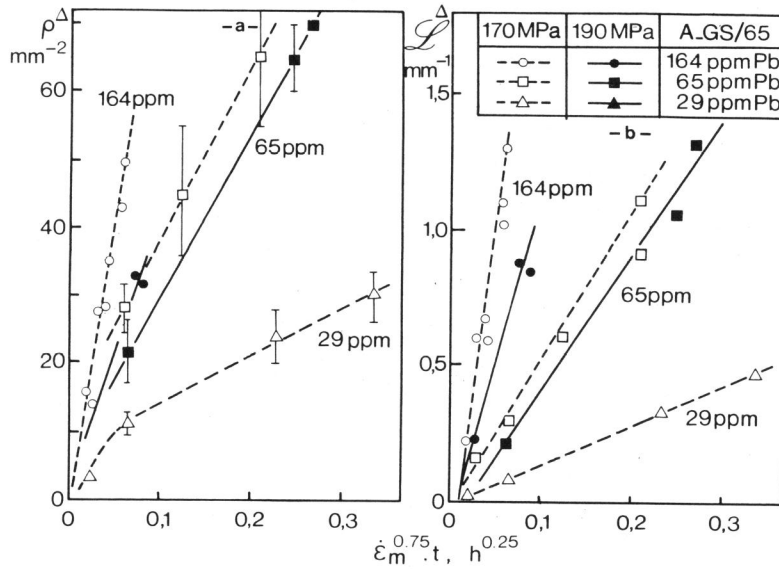


Figure 3 Evolution of total crack density ρ^Δ and length L^Δ in peak-aged alloys with various Pb contents. Time has been corrected for variations in creep rate $\dot{\epsilon}_m$.

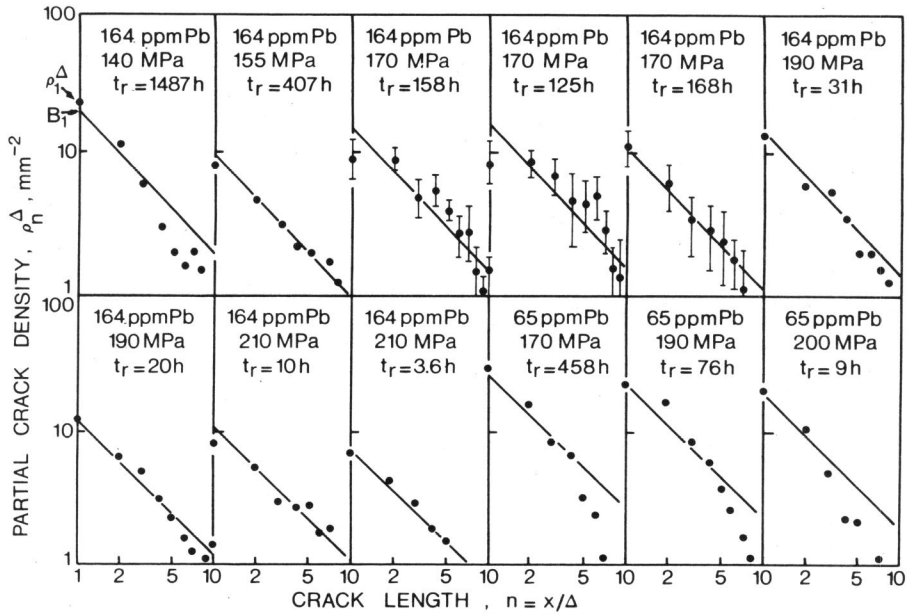


Figure 4 Correlations between measured crack densities and lengths (the slope of all solid lines is $q = 1$).

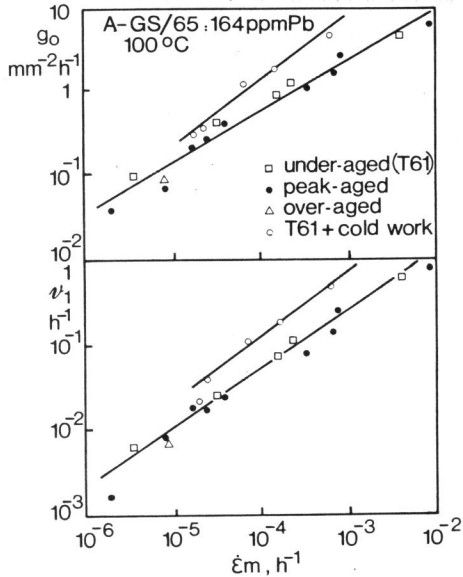


Figure 5 Correlations between g_0 , v_1 and minimum creep rate $\dot{\epsilon}_m$ for all conditions of alloy with 164 ppm Pb.

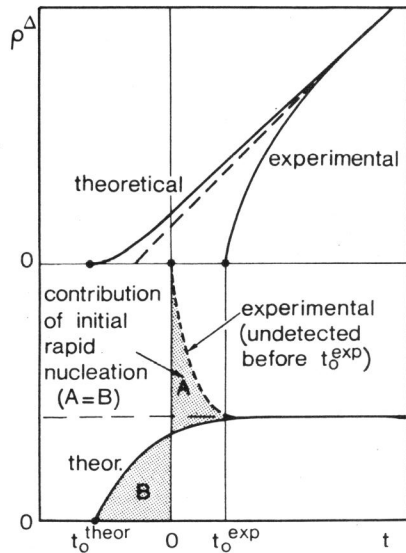


Figure 6 Influence of an initial regime of rapid nucleation superimposed on the solution of the model equations.